Saturn's Periodic Magnetic Field Perturbations are Caused by a Rotating Partial Ring Current

P. C. Brandt,[1] K. K. Khurana,[2] D. G. Mitchell,[1] J. F. Carbary,[1] S. M. Krimigis,[1] B. H. Mauk,[1] C. P. Paranicas,[1] E. C. Roelof,[1] and N. Sergis,[2]

We demonstrate that the periodic magnetic field oscillations observed frequently in Saturn's magnetosphere are caused by an azimuthally asymmetric plasma pressure distribution rotating around Saturn. Plasma pressures inferred from the CAPS (<2 keV), MIMI (>2 keV) and INCA instruments are used to compute the three-dimensional pressure-driven currents and their associated magnetic field perturbations by using the force-balance equation and Biot-Savart integration. While the "cold" (<2 keV) plasma pressure is assumed to be azimuthally symmetric, we show that the observed asymmetric "hot" (> 2 keV) plasma pressure is responsible for the observed magnetic field periodicities.

1. Introduction

Saturn displays periodic signatures observed in Saturn Kilometric Radiation (SKR) [*Kurth et al.*, 2008], charged particles [*Carbary et al.*, 2007], magnetic field [*Giampieri et al.*, 2006], and in energetic neutral atom (ENA) images [*Carbary et al.*, 2008] that are all around the "rotational" period of about 10h39min. The true rotation period of Saturn's core is clouded by the complicated mechanisms that communicates the rotational periodicity throughout the magnetosphere. In this brief paper we explain the mechanism that produces the magnetic field periodicities observed at Saturn and how they relate to the observed ENA periodicities. We show that the periodic magnetic field perturbations are caused by the currents driven by a rotating asymmetric pressure distribution composed of energetic particles - very similar to Earth's partial ring current (PRC), but rotating around the planet. Plasma pressures have been derived from measurements by the Cassini Plasma Spectrometer (CAPS), Low Energy Magnetospheric measurements System (LEMMS), Charge-Mass-Energy Spectrometer (CHEMS) and the Ion-Neutral Camera (INCA) on board Cassini.

It is well established that the terrestrial PRC is extremely dynamic and severely distorts the inner magnetosphere [*Tsyganenko et al.*, 2003]. The terrestrial PRC is composed of energetic protons and O^+, which has

[1]The Johns Hopkins University Applied Physics Laboratory, Laurel, Maryland, USA.

[2]Institute of Geophysics and Planetary Physics, University of California at Los Angeles, Los Angeles, California, USA.

[3]Office for Space Research and Applications, Academy of Athens, Athens, Greece.

0094-8276/08/$5.00

been energized through rapid magnetic field reconfigurations, termed substorms that are especially frequent during strong convection (southward interplanetary magnetic field) [*Krimigis et al.*, 1985; *Hamilton et al.*, 1988; *Fok et al.*, 2006; *Brandt et al.*, 2008]. At Saturn, a similar picture is emerging where the energetic proton and O^+ population is energized in similar processes and is highly asymmetric. As we will show in this paper, Saturn's PRC also perturbs the magnetic field but not as severely as its terrestrial counterpart. However, Saturn's PRC is rotating around the planet due to corotation and magnetic drift, producing a periodic signal in the residual magnetic field data which has led to several hypotheses. *Khurana et al.* [2008] has shown that, qualitatively a rotating PRC and the seasonal plasma sheet tilt is required to explain observations. This paper quantitatively proves that the observed PRC causes the periodic magnetic field perturbations.

We will first describe how we are computing the magnetic field perturbations; secondly, we describe how the "hot" (>2 keV) and "cold" (<2 keV) plasma pressure is derived, and finally we discuss the results and their implications.

2. Computing Field Perturbations

The magnetic field perturbations are computed by solving the force balance equation for the pressure-driven currents in three dimensions in a dipole field. Biot-Savart's law is then used to compute the field perturbation along a given spacecraft trajectory. We neglect the inertial term in the force balance equation since the effect of the centrifugal forces is to stretch the field. As we will see this we lead to a slight offset in the field magnitudes.

In order to arrive at a Biot-Savart integral that is computationally efficient, we follow the approach by *Roelof et al.* [2004] and express the 3D currents in Euler potentials $\mathbf{J} = \nabla\mathbf{Q} \times \nabla\mathbf{P}$, where the second Euler potential Q for a dipole field satisfies $\mathbf{B} \cdot \nabla Q = 1$, so Q is the partial volume of the flux tube (if we set $Q = 0$ at the magnetic minimum-B equator). P is here the pressure, which we assume to be isotropic in this preliminary work. The magnetic field perturbation can then be written

$$\Delta\mathbf{B} = -\mu_\mathbf{0}\mathbf{P}\nabla\mathbf{Q} - \nabla\mathbf{\Psi}, \qquad (1)$$

where our simplified Biot-Savart integral is represented by the scalar function Ψ, which is a function of position $\mathbf{r}$ and the integral is to be taken over all space.

$$-\nabla\Psi = \frac{\mu_0}{4\pi}\int d^3x'\nabla\nabla(\frac{1}{|\mathbf{r'} - \mathbf{r}|})(P\nabla' Q). \qquad (2)$$

Plasma sheet tilt has not been taken into account in this study, but is critical to explain the periodic field signatures observed further out in the tail region [*Khurana et al.*, 2008]. Future work will include plasma sheet tilt.

The idea is now to take time-dependent plasma pressures and evaluate Equation (1) along a given Cassini trajectory. As will be described in more detail below, we assume our cold plasma pressure to be azimuthally symmetric, while the hot plasma pressure is assumed to have the same morphology as the proton distributions derived from global INCA images in the 20-50 keV range and to be rotating with a period of 10.8 h [*Carbary et al.*, 2008].

Although we know that injected energetic particles disperse as they drift around Saturn [*Brandt et al.*, 2008; *Mauk et al.*, 2005], we do not included dispersion in this study. We can do this simplification because our region of interest is in the post midnight sector where injections are fresh and have not undergone significant dispersion. It is important to remember that the injections are *periodic*, which was realized early by *Mitchell et al.* [2005], so that a signficant part of the asymmetric pressure distribution is reenergized every rotation.

3. Plasma Pressure

In order to compute the magnetic field perturbations, realistic estimates of plasma pressures are required. Figure 1 shows statistical *in-situ* measurements of pressure. *Wilson et al.* [2008] has compiled cold (<2 keV) plasma pressures from CAPS, and *Sergis et al.* [2007] has compiled the hot (>2 keV) plasma pressures using data from CHEMS, LEMMS, and INCA (in ion mode). We assume that the cold plasma pressures are azimuthally symmetric, which is a reasonable approximation given the empirical modeling results by *Richardson* [1998]. However, just like the terrestrial PRC [*Brandt et al.*, 2008] it is clear from INCA images that the hot plasma distribution exhibits a very dynamical behavior, where periodic, large-scale injections of energetic particles on the night side drift around the planet [*Mitchell et al.*, 2005; *Brandt et al.*, 2008]. Therefore, we use INCA images obtained at 07:00 UTC DOY 352 2004 to estimate the proton morphology and intensity, as well as phase of the centroid of the asymmetric proton distribution. For simplicity and reasons given above, we assume that the spatial hot plasma pressure distribution is the same as the proton distribution derived from the INCA images.

As is illustrated in Figure 2, we use forward modeling to derive the proton intensity distribution from INCA hydrogen ENA images in the 20-50 keV range. A parametric model of the equatorial proton distribution is used together with a model neutral gas distribution by *Richardson* [1998] to simulate ENA images through the INCA response function. By modifying the parametric proton distribution and keep the neutral gas distribution fixed, until the simulated and observed INCA images agree, we derive the protons intensity distribution. This technique has been extensively used in deriving the global morphology and intensity of Earth's ring current distribution, and also by *Brandt et al.* [2008] for Saturn. Figures 2a and 2b show the final simulated ENA image and the observed INCA image. Figure 2c shows the resulting proton intensity distribution in the equatorial plane.

Next, we use the spectral shapes from the statistical study by *Dialynas et al.* [2008] to compute the total plasma pressure in the 2-200 keV range, as illustrated in Figure 2d. We obtain a maximum "hot" proton pressure around 0.4 nPa using this method.

Hot proton pressures have been determined by *Sergis et al.* [2007], who obtained a *maximum* pressure at about 0.1-0.3 nPa. The *average* pressure is about one order of magnitude lower, but it is critical to keep in mind how dynamic the hot plasma really is at Saturn [*Mitchell et al.*, 2005; *Brandt et al.*, 2008] - something that is well known for Earth (e.g. *Brandt et al.* [2008]). The event analyzed in this paper belongs to one of the stronger "magnetospheric storms" observed by INCA, and given that this strength of storms is statistically rare, it is understandable why such strength is only the upper bound in the *in-situ* statistical study by *Sergis et al.* [2007].

4. Results and Discussion

Figure 3a shows the residual total magnetic field of the modeled perturbations (black line) and the corresponding measured residual field along the Cassini trajectory on DOY 347-358 2004 (Figure 3b). The overall field depression (-38 nT) is caused by the symmetric cold plasma pressure and the periodic perturbations of less than 5 nT amplitude are caused by the rotating hot asymmetric plasma pressure distribution - especially clear on the outbound leg from DOY 351.5 and onward. Figures 3b shows the total (hot + cold) plasma pressure in the equatorial plane with the Cassini trajectory overplotted and the current S/C location indicated by a red circle. Figures 3c and 3d show the simulated and observed INCA hydrogen ENA images in the 20-50 keV range at three different times.

Given the simplicity of our model, it is notable how well the model agrees with observations. The agreement of the periodic perturbations are especially good after DOY 351. This is because we used the INCA images at 07:00 UTC on DOY 351 to derive the morphology and phase of the hot asymmetric pressure distribution. It can be seen that the phase of the periodic perturbations are unclear and different before DOY 349, which is most likely indicative of a larger injection, possibly triggered by a solar wind dynamic pressure increase. This is supported by *Mitchell et al.* [2005] who observed larger injections during the early part of DOY 348. The slight increase in the residual field at about 20:00 UTC on DOY 349 is *not* caused by the asymmetric pressure distribution but appears even only with a symmetric pressure distribution, and is most likely an effect of the 3D character of the orbit.

After about DOY 353 there is an offset between the observed and modeled magnetic field magnitude develops. The measured field maintains its strength to larger distances than what the modeled field does. This can be explained by the stretched field configuration, which we have not accounted for in this study.

We have explained the mechanism behind magnetic field periodicities and how it relates to the periodicity seen in large-scale injections, but the question of where the periodicity ultimately comes from is still left unsolved. Observational evidence is mounting in support for plasmoid release [*Hill et al.*, 2008; *Jackman et al.*, 2007] as the common driver for periodic phenomena in INCA, MAG, and SKR. We believe that there is sufficient evidence for proposing that *periodic plasmoid release* is indeed the driver of all observable magnetospheric periodic phenomena. The underlying cause of the periodic plasmoid release itself could be that this is the natural frequency of the mass-loaded magnetosphere-ionosphere system resulting from requiring balance between cold plasma source and the plasma loss down the tail. No longitudinal anomalies in ionospheric conductance or magnetic field have been observed so far, but they are also natural candidates to explain the periodicity. We will develop our hypothesis in a future paper. Nevertheless, it is clear that a physics-based model is highly needed to reveal the planetary rotation that is hidden behind the periodic phenomena observed in the magnetosphere.

5. Summary and Conclusions

We have shown that the observed magnetic field periodicities in Saturn's magnetosphere are caused by a hot (>2 keV) rotating asymmetric pressure distribution - a partial ring current. The source and distribution of the pressure driving the PRC is consistent with the periodic hot plasma injection as observed by INCA [*Mitchell et al.*, 2005; *Carbary et al.*, 2008; *Brandt et al.*, 2008]. The dominating depression is caused by the symmetric cold plasma pressure observed by *Wilson et al.* [2008].

In order to compute the magnetic field perturbations we solved the force-balance equation, neglecting centrifugal forces, and assuming isotropic pressure. A modified Biot-Savart integration was then used to reproduce the magnetic field perturbations along the Cassini trajectory on DOY 347-358 2004. Cold (<2 keV) and hot (>2 keV) plasma pressures were obtained from CAPS measurements [*Wilson et al.*, 2008], and from a combination of CHEMS, LEMMS *in-situ* measurements and remote global ENA images obtained from INCA to determine the instantaneous global spatial distribution and phase of the hot asymmetric plasma pressure.

This work represents a step towards revealing the true planetary rotation period by determining the mechanisms that relate different periodic phenomena in Saturn's magnetosphere. We believe that the next step should be to explain the close relation between the periodic SKR signals and the periodic large-scale injections.

Acknowledgments. This work was supported by NASA Grant NNX07AJ69G. Thanks to H. McAndrews and R. Wilson for providing cold plasma pressures.

References

Brandt, P. C., C. P. Paranicas, J. F. Carbary, D. G. Mitchell, B. H. Mauk, and S. M. Krimigis, Understanding the global evolution of Saturn's ring current, *Geophys. Res. Lett.*, *35*, 17,101–+, doi:10.1029/2008GL034969, 2008.

Brandt, P. C., Y. Zheng, T. S. Sotirelis, K. Oksavik, and F. J. Rich, The linkage between the ring current and the ionosphere system, *AGU Geophysical Monograph*, in press, 2008.

Carbary, J. F., D. G. Mitchell, S. M. Krimigis, D. C. Hamilton, and N. Krupp, Charged particle periodicities in Saturn's outer magnetosphere, *Journal of Geophysical Research (Space Physics)*, *112*(A11), 6246–+, doi:10.1029/2007JA012351, 2007.

Carbary, J. F., D. G. Mitchell, P. Brandt, C. Paranicas, and S. M. Krimigis, ENA periodicities at Saturn, *Geophys. Res. Lett.*, , *35*, 7102–+, doi:10.1029/2008GL033230, 2008.

Dialynas, K., S. Krimigis, D. Mitchell, N. Krupp, and P. Brandt, Energetic ion spectral characteristics in the saturnian magnetosphere using cassini/mimi measurements, *J. Geophys. Res.*, in press, 2008.

Fok, M. C., T. E. Moore, P. C. Brandt, D. C. Delcourt, S. P. Slinker, and J. A. Fedder, Impulsive enhancements of oxygen ions during substorms, *J. Geophys. Res.*, *111*, doi:10.1029/2006JA011839, 2006.

Giampieri, G., M. K. Dougherty, E. J. Smith, and C. T. Russell, A regular period for Saturn's magnetic field that may track its internal rotation, *Nature*, *441*, 62–64, doi:10.1038/nature04750, 2006.

Hamilton, D. C., G. Gloeckler, F. M. Ipavich, W. Studemann, B. WIlken, and G. Kremser, Ring current development during the great geomagnetic storm of February 1986, *J. Geophys. Res.*, *93*(A12), 14,343–14,355, 1988.

Hill, T. W., et al., Plasmoids in Saturn's magnetotail, *Journal of Geophysical Research (Space Physics)*, *113*(A12), 1214–+, doi:10.1029/2007JA012626, 2008.

Jackman, C. M., C. T. Russell, D. J. Southwood, C. S. Arridge, N. Achilleos, and M. K. Dougherty, Strong rapid dipolarizations in Saturn's magnetotail: In situ evidence of reconnection, *Geophys. Res. Lett.*, , *34*, 11,203–+, doi: 10.1029/2007GL029764, 2007.

Khurana, K. K., D. G. Mitchel, C. S. Arridge, M. K. Dougherty, C. T. Russell, C. Paranicas, and N. Krupp, The mystery of rotational signals in saturns magnetosphere, *J. Geophys. Res.*, in review, 2008.

Krimigis, S. M., G. Gloeckler, R. W. McEntire, T. A. Potemra, F. L. Scarf, and E. G. Shelley, Magnetic storm of September 4, 1984: A synthesis of ring current spectra and energy densities measured with AMPTE/CCE, *Geophys. Res. Lett.*, *12*(5), 329–332, 1985.

Kurth, W. S., T. F. Averkamp, D. A. Gurnett, J. B. Groene, and A. Lecacheux, An update to a Saturnian longitude system based on kilometric radio emissions, *Journal of Geophysical Research (Space Physics)*, *113*(A12), 5222–+, doi: 10.1029/2007JA012861, 2008.

Mauk, B. H., et al., Energetic particle injections in saturns magnetosphere, *Geophys. Res. Lett.*, *32*(L14S05), doi: 10.1029/2005GL022485, 2005.

Mitchell, D. G., et al., Energetic ion acceleration in Saturn's magnetotail: Substorms on Saturn?, *Geophys. Res. Lett.*, *32*(L20S01), doi:10.1029/2005GL022647, 2005.

Richardson, J. D., Thermal plasma and neutral gas in Saturn's magnetopshere, *Rev. of Geophys.*, *36*(4), 501–524, 1998.

Roelof, E. C., P. C. Brandt, and D. G. Mitchell, Derivation of currents and diamagnetic effects from global pressure distributions obtained by IMAGE/HENA, *Adv. Space Res.*, *33/5*, 747–751, doi:10.1016/S0273-1177(03)00633-1, 2004.

Sergis, N., S. M. Krimigis, D. G. Mitchell, D. C. Hamilton, N. Krupp, B. M. Mauk, E. C. Roelof, and M. Dougherty, Ring current at Saturn: Energetic particle pressure in Saturn's equatorial magnetosphere measured with Cassini/MIMI, *Geophys. Res. Lett.*, , *34*, 9102–+, doi: 10.1029/2006GL029223, 2007.

Tsyganenko, N. A., H. J. Singer, and J. C. Kasper, Stormtime distortion of the inner magnetosphere: How severe can it get?, *Journal of Geophysical Research (Space Physics)*, *108*, 1209–+, doi:10.1029/2002JA009808, 2003.

Wilson, R. J., R. L. Tokar, M. G. Henderson, T. W. Hill, M. F. Thomsen, and D. H. P. Jr, Cassini plasma spectrometer thermal ion measurements in saturn's inner magnetosphere, *J. Geophys. Res.*, doi:10.1029/2008JA013486, in press, 2008.

P. C. Brandt, The Johns Hopkins University Applied Physics Laboratory, 11100 Johns Hopkins Rd, Laurel, MD 20723, USA. (pontus.brandt@jhuapl.edu)

K. K. Khurana, Institute of Geophysics and Planetary Physics, University of California at Los Angeles Los Angeles, CA 90095, USA. (kkhurana@igpp.ucla.edu)

D. G. Mitchell, The Johns Hopkins University Applied Physics Laboratory, 11100 Johns Hopkins Rd, Laurel, MD 20723, USA. (don.mitchell@jhuapl.edu)

J. F. Carbary, The Johns Hopkins University Applied Physics Laboratory, 11100 Johns Hopkins Rd, Laurel, MD 20723, USA. (james.carbary@jhuapl.edu)

S. M. Krimigis, The Johns Hopkins University Applied Physics Laboratory, 11100 Johns Hopkins Rd, Laurel, MD 20723, USA. (tom.krimigis@jhuapl.edu)

B. H. Mauk, The Johns Hopkins University Applied Physics Laboratory, 11100 Johns Hopkins Rd, Laurel, MD 20723, USA. (barry.mauk@jhuapl.edu)

C. P. Paranicas, The Johns Hopkins University Applied Physics Laboratory, 11100 Johns Hopkins Rd, Laurel, MD 20723, USA. (chris.paranicas@jhuapl.edu)

E. C. Roelof, The Johns Hopkins University Applied Physics Laboratory, 11100 Johns Hopkins Rd, Laurel, MD 20723, USA. (ed.roelof@jhuapl.edu)

N. Sergis, Office for Space Research and Applications, Academy of Athens, Athens, Greece. (nsergis@phys.uoa.gr)

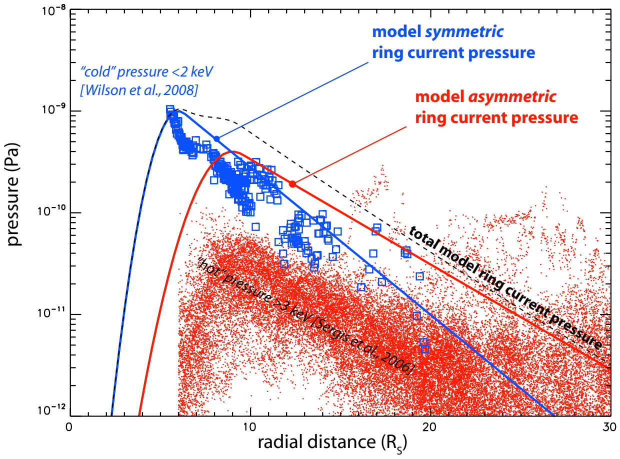

Figure 1. Cold (<2 keV) symmetric plasma pressure (solid blue line) was derived from CAPS measurements by *Wilson et al.* [2008] (blue squares). The distribution and phase of the hot asymmetric pressure distribution (solid red line) was derived from global INCA images and *in-situ* ion spectra by *Dialynas et al.* [2008]. The statistical distribution of the hot plasma pressure obtained from *in-situ* by *Sergis et al.* [2007] is shown for comparison (red dots).

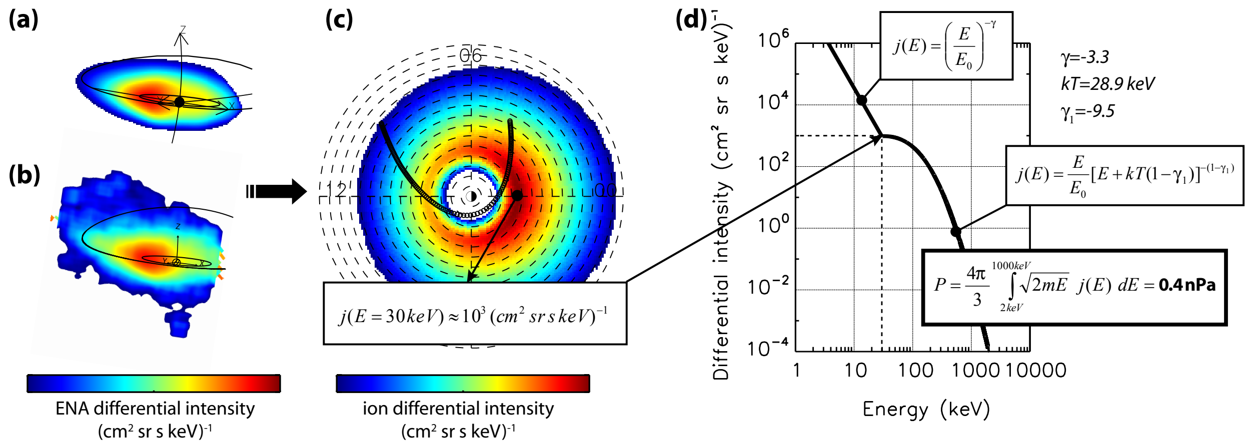

Figure 2. A parametric proton distribution is used to simulate INCA images (a) until the match the observations at 07:00 UTC DOY 352 2004 (b). The resulting proton distribution (c) provides us with the spatial distribution, phase and intensity. *In-situ* proton spectra by *Dialynas et al.* [2008] are then used to compute the hot plasma pressure (d).

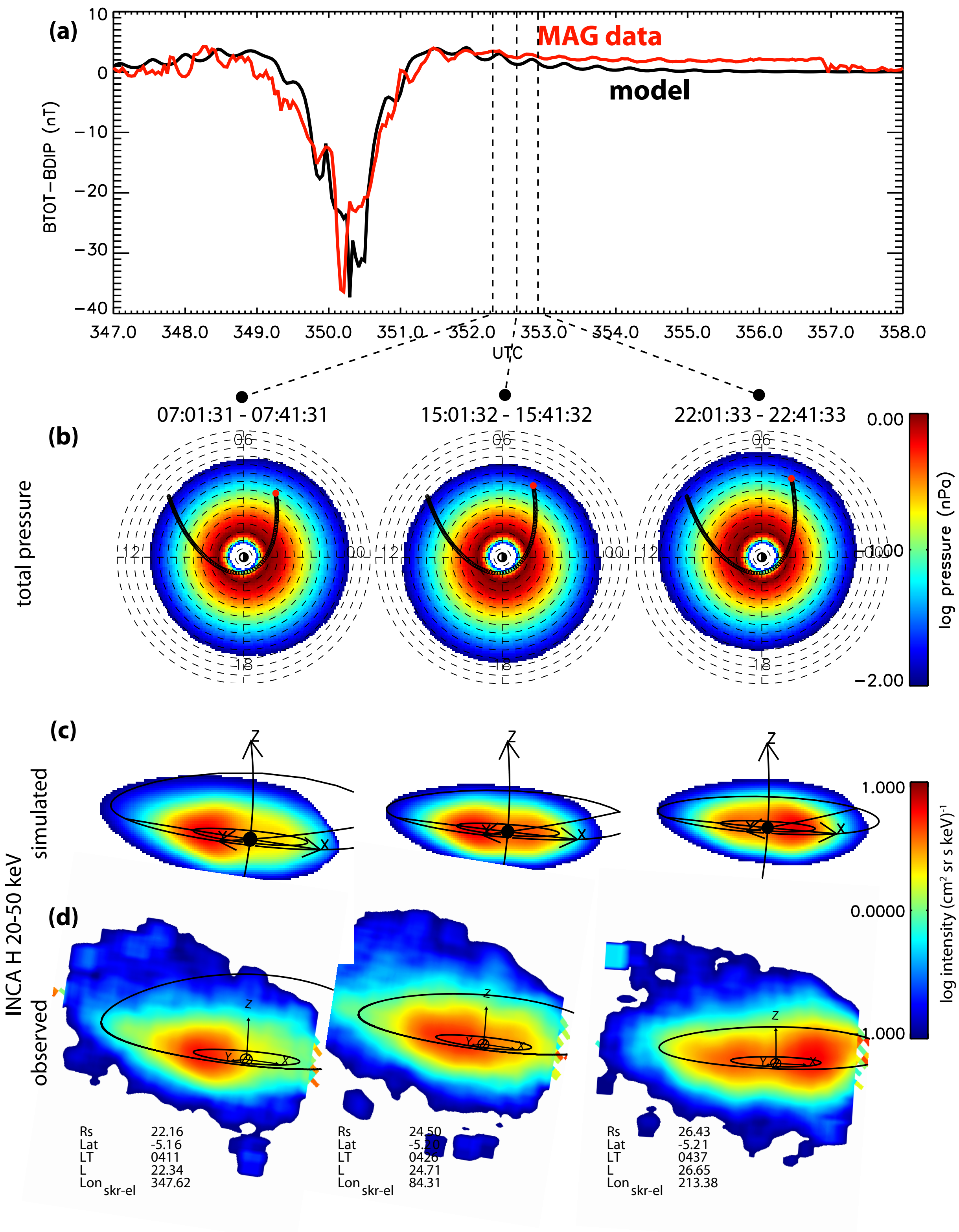

Figure 3. A compilation of the model results. (a) Measured residual field strength (red) and modeled field. (b) The total pressures (hot + cold) in the equatorial plane used in the magnetic field calculation with the projected Cassini trajectory in black with the current S/C/ location marked by the red circle. (c) The simulated ENA images of the 20-50 keV proton distribution (also shown in Figure 2) and (d) the corresponding observed INCA hydrogen images.